RECAPP-HRI-2014-002

Right Sneutrino Dark Matter and a Monochromatic Photon Line

Arindam Chatterjee,[1,*] Debottam Das,[2,†]
Biswarup Mukhopadhyaya,[1,‡] and Santosh Kumar Rai[1,§]

[1] *Regional Centre for Accelerator-based Particle Physics,*
Harish-Chandra Research Institute, Chhatnag Road, Jhusi, Allahabad 211019, India

[2] *Institut für Theoretische Physik und Astrophysik,*
Universität Würzburg, Am Hubland, 97074 Würzburg, Germany

arXiv:1401.2527v1 [hep-ph] 11 Jan 2014

Abstract

The inclusion of right-chiral sneutrino superfields is a rather straightforward addition to a supersymmetric scenario. A neutral scalar with a substantial right sneutrino component is often a favoured dark matter candidate in such cases. In this context, we focus on the tentative signal in the form of a monochromatic photon, which may arise from dark matter annihilation and has drawn some attention in recent times. We study the prospect of such a right sneutrino dark matter candidate in the contexts of both MSSM and NMSSM extended with right sneutrino superfields, with special reference to the Fermi-LAT data.

Keywords: Supersymmetry, Dark Matter, Right sneutrino

* Email: arindam@hri.res.in
† Email: debottam.das@physik.uni-wuerzburg.de
‡ Email: biswarup@hri.res.in
§ Email: skrai@hri.res.in

I. INTRODUCTION

Various observations ranging from galactic rotation curves to the observed anisotropy in the cosmic microwave background radiation, have strengthened our belief in a substantial cold Dark Matter (DM) component of the universe. It is therefore hardly surprising that, side by side with direct searches, all indirect evidences of dark matter are also of great interest.

Analyses of the publicly available Fermi-LAT [1] data found a tentative hint through an observation of a γ-ray line at ~ 130 GeV coming from the vicinity of the galactic center [2–5]. In ref. [3] it was shown that a possible explanation for such a γ-ray line could be via DM pair annihilations into two photons, with a DM mass of $129.8 \pm 2.4^{+7}_{-13}$ GeV and annihilation cross-section $\langle \sigma v \rangle_{\gamma\gamma} = \left(1.27 \pm 0.32^{+0.18}_{-0.28}\right) \times 10^{-27} \mathrm{cm}^3 \mathrm{s}^{-1}$ [4–11]. Moreover, there is a faint indication (1.4σ) of two lines which can be extracted from the Fermi data, one at ~ 130 GeV and a weaker one at ~ 114 GeV [5, 12]. Such a pair of lines can be naturally explained by a DM particle of mass ~ 130 GeV annihilating into $\gamma\gamma$ and γZ with a relative annihilation cross-section $\langle \sigma v \rangle_{\gamma Z} / \langle \sigma v \rangle_{\gamma\gamma} = 0.66^{+0.71}_{-0.48}$ [13]. Though there is no well-accepted astrophysical process that can explain the γ-ray line, doubts have been raised [14, 15] to its line feature by making it compatible with a diffuse background. Preliminary analysis of the Fermi-LAT Collaboration also confirms a line feature around ~ 133 GeV but with a lower statistical significance [16] and concluded that more data would be required to establish the origin of such a feature.

Following reference [3], various models have been proposed to explain the monochromatic feature of the γ-ray, see e.g. [17–48]. Most models are further constrained from the continuum flux of photons arising from annihilations of the DM into W and Z bosons and the Standard Model (SM) fermions [23, 41–44]. Supersymmetric (SUSY) theories with a viable cold DM candidate have been well studied in this context. However it is found that within the minimalistic versions where the lightest neutralino is the DM candidate, it is very difficult to accommodate the γ-ray line signal. We can summarize the shortcomings as follows:

- In the minimal version, *viz.* the Minimal Supersymmetric Standard Model (MSSM), it is difficult to obtain the large annihilation cross-section of neutralino pairs into photons $\langle \sigma v \rangle_{\gamma\gamma}$ [49], while satisfying constraints imposed by the thermal relic density and large continuum flux [22] data.

- In the Next-to-Minimal Supersymmetric Standard Model (NMSSM), which addresses the μ-problem in MSSM, one can accommodate the large annihilation cross-section of the neutralino pairs into photons by exploiting the *very* singlet like CP-odd Higgs boson resonance [40, 50, 51]. However, the parameter space is tightly constrained by the direct searches for the DM, most importantly by the data from XENON100 and LUX [52, 53]. It is however observed that in a specific region of the parameter space, where $\mu_{eff} < 0$, constraints from direct detection can be relaxed by an order, in compliance with the bound from XENON100 [45].

In addition, a 130 - 135 GeV photon signal can be produced both in the the MSSM and the NMSSM through internal bremsstrahlung [47, 54], although a a significant boost factor is required [47] in the latter scenario.

In this work we study the feasibility of a new DM candidate, *viz.* a right-chiral sneutrino, $\tilde{\nu}_R$ (with some degree of mixing with a left-chiral one), as the candidate for producing the photon line. The simplest way to accommodate non-zero (Dirac) neutrino masses in SUSY models is by introducing a right-handed singlet neutrino. This would entail addition of right-chiral neutrino superfields in the MSSM*. In addition we ensure that the thermal relic density is in agreement with WMAP data [55] and also satisfies constraints from DM-nucleus scattering [52, 53]. Thanks to their singlet nature, the right-handed sneutrinos ($\tilde{\nu}_R$), acting as cold DM candidates [56–58] in the MSSM, can account for all tentative evidences of DM we have so far. A sizeable volume of work has also taken place on the LHCs signals of (right) sneutrino DM [59], and also on the related scenarios carrying implications on different aspects of phenomenology [60, 61]. However, as we will discuss, a 130-135 GeV $\tilde{\nu}_R$ DM, that can produce $\langle\sigma v\rangle_{\gamma\gamma} \sim 1.2 \times 10^{-27}$, falls short in accounting for all the continuum constraints.

To get around this difficulty, we consider a similar scenario in the Next-to-Minimal Supersymmetric Standard Model ($\tilde{\nu}_R$NMSSM) with a scale invariant superpotential, assuming a $\tilde{\nu}_R$ type DM. Notably, $\tilde{\nu}_R$ can naturally acquire a Majorana mass term of $\mathcal{O}(1)$ TeV. In addition to contributing neutrino masses and mixings [62, 63], $\tilde{\nu}_R$ DM in the NMSSM may have rich phenomenology as discussed in ref: [64–67]. As will be discussed in detail, in this

* In the standard seesaw extensions of MSSM, Majorana mass scale for the right handed neutrino superfields is very close the gauge coupling unification scale ($M_G \sim 10^{16}$ GeV) which makes right handed sneutrinos very massive (close to M_G), thus not suitable for electro-weak scale dark matter candidate.

case, one can even evade the continuum constraints when considering resonant annihilation mediated via a singlet-like Higgs boson. Additionally, the constraints from XENON100 and LUX on the spin-independent direct detection cross–section can also be satisfied.

This paper is organized as follows: in Section II we discuss resonant annihilation of DM; following which, in Section III, we explore the possibility of explaining the observed γ signal with $\tilde{\nu}_R$ DM in the MSSM and the NMSSM. Finally, we summarize in Section IV.

II. BREIT-WIGNER RESONANCE: EFFECT OF THRESHOLD

The pair annihilation of $\tilde{\nu}_R$ into two photons can proceed via a dominantly singlet/doublet like CP-odd (CP-even) Higgs A (H) in the s-channel. Before getting into specific models,

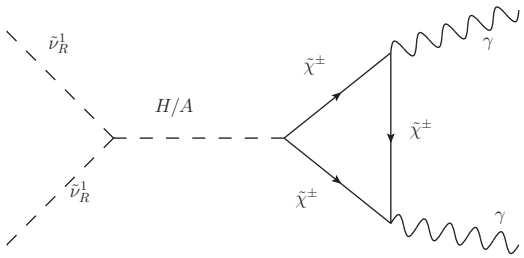

FIG. 1. The dominant annihilation diagram for $\tilde{\nu}_R$–like DM into two photons via a singlet–like CP-even/CP-odd Higgs H/A in the NMSSM. Similar diagrams with (s)quarks and (s)leptons running in the loop contribute negligibly.

we first discuss the annihilation of a spin-0 dark matter particle ($\tilde{\nu}_R$ in our context) with mass m, mediated via a spin-0 particle of mass M near the resonance. DM annihilations near resonances and thresholds have been previously studied [68–70]. Our discussion closely follows [69, 70].

The cross–section of an s–channel scattering process, near the resonance, is given by,

$$\sigma = \frac{32\pi}{4E_1E_2v\overline{\beta_i}}\frac{M^2\Gamma^2}{(s-M^2)^2+M^2\Gamma^2}B_iB_f, \tag{1}$$

where $\overline{\beta_i} = \sqrt{1-\frac{4m^2}{M^2}}$; B_i and B_f are the branching fractions of the intermediate particle into the initial and final channels respectively and Γ is the total decay width of the same; E_1 and E_2 are the energies of the two annihilating particles; $s = (p_1+p_2)^2$ where p_1 and p_2 represent the four-momenta of the two annihilating particles. In the thermal averaging of

σv, in the context of DM, the Møller velocity (v) is used [68]. However, in the rest frame of one of the annihilating particles, and also in the center of momentum (CM) frame, the Møller velocity is reduced to the relative velocity of these particles. Following Ref. [69], to quantify the resonance, an auxiliary parameter δ is introduced, such that,

$$M^2 = 4m^2(1-\delta)\ . \tag{2}$$

Since, in the present context, the annihilating particles in resonance are non-relativistic, $|\delta| \ll 1$ is assumed. Note that for $\delta < 0$, a physical pole ($s = M^2$) is encountered when $v \simeq 2\sqrt{|\delta|}$ (in the CM frame, where v denotes the magnitude of the relative velocity of the annihilating particles); while, for $\delta > 0$, a physical pole is never encountered. In the former situation $B_i,\ B_f$ are well–defined, consequently Eq. (1) holds good in this region. However, in the latter ($\delta > 0$), the intermediate particle can no longer decay into two dark matter particles; consequently B_i and $\overline{\beta_i}$ are unphysical (imaginary numbers). However, $B_i/\overline{\beta_i}$ remains well-defined. In this case, Eq. 1 can also be expressed as,

$$\sigma = \frac{2|C|^2}{4E_1E_2v}\frac{M\Gamma}{(s-M^2)^2+M^2\Gamma^2}B_f\ , \tag{3}$$

where, C denotes the coupling between dark matter particles and the mediating particle which in our context are $\tilde{\nu}_R$ and the CP-even or CP-odd Higgs respectively. In the CM frame, with non-relativistic dark matter particles ($v \ll 1$), we have $s \equiv 4m^2(1+v^2/4)$. Eq. 1, then, reduces to [69],

$$\sigma v = \frac{32\pi}{M^2}\frac{\gamma^2 B_f}{(\delta+v^2/4)^2+\gamma^2}\Big(\frac{B_i}{\overline{\beta_i}}\Big), \tag{4}$$

where $\gamma = \Gamma/M$.

In the limit of narrow width resonance $\gamma \ll 1$ while for max $(|\delta|,\gamma) < v \ll 1$ the denominator of Eq. 4 receives dominant contribution from v^2, and thus σv is enhanced as v decreases. This behavior continues until $v \lesssim$ max $(|\delta|,\gamma)$. Finally, for $v \ll$ max $(|\delta|,\gamma)$, σv becomes insensitive to v, and is then determined only by δ and γ. On the contrary, in case of broad width resonance ($\gamma \gg 1$), with $\gamma \gg$ max $(|\delta|, v^2/4)$ and $v \ll 1$), γ^2 dominates in the denominator, and thus $\gamma^2/((\delta+v^2/4)^2+\gamma^2) \simeq 1$.

Since DM annihilation into $\gamma\gamma$, in our case, is a loop–suppressed process, the required $\langle\sigma(\tilde{\nu}_R\tilde{\nu}_R \to \gamma\gamma)v\rangle \simeq 10^{-27}$ cm^3 s^{-1} apparently leads to a larger $\langle\sigma_{ann}v\rangle$, where σ_{ann} denotes the total annihilation cross–section of the DM into the SM particles. As all the tree-level

processes are mediated by the same intermediate state (at resonance), it leads to a much lower thermal relic abundance. We therefore now discuss about how we achieve the required cross–sectio $\langle\sigma v\rangle$ for the γ signal, as well as the correct relic abundance.

- In the context of the γ signal, $\langle\sigma v\rangle$ annihilation cross–section needs to be evaluated at late times, i.e. typically when $v_{rel} \sim 0.001$. Thus, in Eq. 4, with $|\delta| \sim \mathcal{O}(10^{-2})$, v can be ignored in the denominator. As we shall discuss in the next section, by suitably choosing the coupling C (as in Eq. 3) along with δ, γ, it is possible to achieve the required cross–section in the $\tilde{\nu}_R$NMSSM.

- During freeze-out, away from a pole, the typical velocity of cold DM is about 0.3. Here, by freeze-out, we mean when $(n - n_{eq}) \simeq n_{eq}$; n and n_{eq} represent the DM density at a given time/temperature and the equilibrium value of the same respectively. Let the corresponding freeze-out temperature be denoted by T_f. [†] Since after freeze-out (in the absence of a pole) annihilations do not affect the relic abundance of DM significantly, the abundance at T_f usually provides a good estimate of relic abundance. Since DM is non-relativistic at freeze-out, the thermal abundance at T_f is exponentially suppressed by a factor $x_f = \dfrac{m}{T_f}$. The situation is different for the two regions in the vicinity of the pole, namely, $\delta > 0$ and $\delta < 0$.

  □ When $\delta > 0$ (a scenario consistent with narrow width resonance), in the region $v^2 > 4$ max $(\delta,\ \gamma)$, the cross–section σ is dominated by γ/v^2. Thus, $\langle\sigma v\rangle$, at a temperature $T \sim m v_0^2$, $v_0^2 \gg$ max $(\delta,\ \gamma)$, is determined by γ/v_0^2. At such large v_0, $s > M^2$, and thus annihilations dominantly occur further away from the pole, and may have cross–sections similar to the other annihilation channels (if allowed) not mediated via the resonance. However, as T, and therefore v_0, decreases, the annihilation channels mediated via the resonance tend to have larger $\langle\sigma v\rangle$, and thus, do not decouple. Consequently DM can continue to annihilate through these channels until $v_0^2 < 4$ max $(\delta,\ \gamma)$. After that, the corresponding σ does not change any more, and, assuming that these are the only annihilation channels, the relic density would be determined by δ and γ only. [69].

[†] We have used `micrOMEGAs` to obtain the freeze-out temperature, and also the relic abundance. Note that, `micrOMAGAs` uses $n(T_f) = 2.5\ n_{eq}(T_f)$ to estimate the freeze-out temperature T_f[71].

□ For $\delta < 0$, the pole is physical. Therefore, unlike the previous case, at $s = M^2$ or $v^2 \simeq 4|\delta|$, σ is very large. At high temperatures, $T \sim m|\delta|$, $\langle\sigma v\rangle$ is large, and then decreases with T. Thus, in this case, the annihilation channels mediated via the resonance decouple early. Consequently, the relic density of the DM, at late times, remain similar to a scenario where DM has a similar annihilation cross-section even without the resonance [69]. For smaller values of $|\delta|$ and γ a large boost factor (defined as $\frac{\langle\sigma v\rangle|_{T\to 0}}{\langle\sigma v\rangle|_{T\sim T_f}}$) can be obtained in this case too [70].

- The time of freeze-out, while a little away from the pole, also has a moderate dependence on the coupling C (see Eq. 3). When $\delta > 0$, for large v_0, such that $v_0^2 \gtrsim 4\ \max(\delta,\ \gamma)$ the contribution from the resonant annihilation can be small compared to H, and freeze-out can happen early compared to a similar scenario (i.e. with similar value of C) with $\delta < 0$. In the former scenario, the resonant channel decouples much late (i.e. when $\Gamma \leq H$, where Γ and H denote the interaction rate with the thermal soup and the Hubble expansion rate respectively) as its contribution continues to increase until $v_0^2 \lesssim 4\ \max(\delta,\ \gamma)$. But this late decoupling does not lead to exponential suppression (by $x_D = \dfrac{m}{T_D}$, where T_D is the decoupling temperature) to the relic density. On the other hand, large annihilation cross–section at high v_0 leads to large contribution to the thermally averaged annihilation cross-section at early times for $\delta < 0$. This, in turn, results in late freeze-out and a lower relic abundance [69]. As we will elaborate in the next section, for our benchmark points, we could obtain large relic in the former scenario, i.e. with $\delta > 0$. On the other hand, since DM annihilations into two photons happens at late time, even with $\delta > 0$ it is possible to obtain the required $\langle\sigma v\rangle_{\gamma\gamma}$.

III. PHOTON SIGNAL WITH $\tilde{\nu}_R$ DARK MATTER

In the following, we discuss the different avenues of indirect detections for a relatively light $\tilde{\nu}_R$ dark matter focusing on the γ ray line observed at $E_\gamma \sim 130 - 135$ GeV. As mentioned earlier, we extend the MSSM and the NMSSM with three generations of right handed neutrino superfields ($\hat{\nu}_R^c$). Assuming that the $\tilde{\nu}_R^c$ is the lightest SUSY particle (LSP) in the supersymmetric particle spectrum, we enforce that the following phenomenological constraints always hold.

- A relic density complying with the WMAP bound $\Omega h^2 = 0.1120 \pm 0.011$ [55] (with 2σ error bars).

- A SM-like Higgs boson with $M_{H_{SM}} = 124 - 127$ GeV.

- Constraints from B-physics which has little impact for the $\tan\beta$ considered here.

- Upper bounds on annihilation cross sections into W^+W^-, ZZ, $b\bar{b}$ and $\tau\bar{\tau}$ channels from the Fermi LAT collaboration [72, 73], as well as bounds from PAMELA on the anti-proton flux [74].

For exact calculation of the sneutrino mass and mixing matrices as well as two-loop renormalization group equations (RGEs) for all SUSY parameters, we have used the publicly available code called `SARAH` [75]. These RGEs are then implemented in the software package `SPheno` [76] for numerical evaluation of all physical parameters and phenomenological constraints. For computation of relic density, all indirect detection cross–sections and fluxes, we implement `SARAH` generated `CalcHEP` [77] model files into `micrOMEGAs` [71]. We however calculate the cross-section for the photon line $\langle\sigma v\rangle_{\gamma\gamma}$ signal with our own mathematica code based on Ref. [69, 70]. We ignore the contribution of $\langle\sigma v\rangle_{\gamma\gamma}$ in the relic density computation.

In both the models that we have considered, we scan the parameter space while keeping the soft SUSY breaking terms in the following preferred ranges.

- Squark masses of 2-3 TeV are assumed to alleviate LHC constraints from direct SUSY searches. The latter choice also helps to enhance the lightest Higgs boson mass irrespective of the choice of $\tan\beta$. Similarly, gluino masses (M_G) is fixed around ~ 2 TeV. The slepton masses are assumed to be around 300 GeV to have consistent spectra with muon anomalous magnetic moment.

- Trilinear soft susy breaking terms $T_t = -3$ TeV and $T_b = -1.0$ TeV (scaled with the Yukawa couplings).

- We use $m^2_{\tilde{\nu}_R}$ as free parameter. Similarly, the couplings y_ν and T_ν for $\nu_l - \nu_R$ and $\tilde{\nu}_l - \tilde{\nu}_R$ are assumed flavor diagonal. In the present context, we refrain from exact calculation of neutrino masses and mixing angles.

- $\mu \sim \pm(200 - 300)$ GeV is assumed.
- We have used the top quark pole mass $m_{\rm top} = 173.1$ GeV.

A. $\tilde{\nu}_R$ and the MSSM

In this section, we discuss the status of $\tilde{\nu}^c_R$ dark matter in the (R-parity conserving) MSSM with three generations of right-handed (s)neutrinos. The neutrino masses arise from the Yukawa interaction only (*purely Dirac-type*) and can be obtained from the following superpotential:

$$W = W_{MSSM} + y_\nu \, \hat{H}_u \cdot \hat{L} \, \hat{\nu}^c_R \,, \tag{5}$$

where W_{MSSM} denotes the MSSM superpotential; $\hat{H}_u$, $\hat{L}$ and $\hat{\nu}^c_R$ represents the up-type Higgs, lepton doublet and right-handed neutrino superfields respectively. For simplicity, we consider all mass and coupling parameters to be real and suppress flavor indices for neutrino families. Assuming soft-supersymmetry breaking, as in the MSSM, the soft-breaking scalar potential becomes,

$$V_{soft} = V_{MSSM} + (T_\nu \, H_u \cdot \tilde{L} \, \tilde{\nu}^c_R + \text{h.c.}) + m^2_{\tilde{\nu}_R} |\tilde{\nu}^c_R|^2 \,, \tag{6}$$

where V_{MSSM} denotes the soft-supersymmetry breaking terms in the MSSM and soft trilinear coupling is given by $T_\nu \equiv T_{\nu_\alpha} y_{\nu_\alpha}$, where α denotes the generation index. Neutrino masses can be expressed as,

$$m_\nu = y_\nu \, \langle H^0_u \rangle = y_\nu \, \frac{v}{\sqrt{2}} \, \sin\beta \tag{7}$$

where $v \simeq 246$ GeV is the vacuum expectation value (VEV) of the standard-model -like Higgs boson, and $\tan\beta = \langle H^0_u \rangle / \langle H^0_d \rangle$. Clearly, neutrino masses ($m_\nu \sim 0.1$ eV) put constraints on the size of the neutrino Yukawa couplings $y_\nu \sim \mathcal{O}(10^{-12})$. Ignoring flavor mixing in the $\tilde{\nu}$ sector [‡] the (2×2) mass matrix for $\tilde{\nu}_\alpha$ for any flavor α, can be written as,

$$m^2_{\tilde{\nu}_\alpha} = \begin{pmatrix} m^{\alpha 2} & \frac{1}{\sqrt{2}} \Big(- v_d \, \mu \, y^*_{\nu_\alpha} + v_u T^*_{\nu_\alpha} \Big) \\ \frac{1}{\sqrt{2}} \Big(- v_d \, \mu^* \, y_{\nu_\alpha} + v_u T_{\nu_\alpha} \Big) & \frac{1}{2} v^2_u |y_{\nu_\alpha}|^2 + m^2_{\tilde{\nu}_{R\alpha}} \end{pmatrix} \tag{8}$$

[‡] Although flavor violation cannot be ignored in the ν sector, in $\tilde{\nu}$ sector, it is only induced through terms proportional to y_ν, assuming the soft-breaking terms to be flavor conserving. Since y_ν is $\mathcal{O}(10^{-12})$, such effects are very small and do not affect our results.

with

$$m^{\alpha 2} = \frac{1}{8}\Big(4v_u^2|y_{\nu_\alpha}|^2 + 8m_{\tilde{l}_\alpha}^2 + \Big(g_1^2 + g_2^2\Big)\Big(- v_u^2 + v_d^2\Big)\Big), \tag{9}$$

where $m_{\tilde{l}_\alpha}$ is the soft breaking term for $\tilde{l}_\alpha$. The lightest sneutrino mass eigenstates $\tilde{\nu}_R^1$, as obtained after diagonalization of $\tilde{\nu}_\alpha$, can be a valid candidate for DM. Moreover, such a $\tilde{\nu}_R^1$ can also produce viable photon signal $\langle\sigma v\rangle_{\gamma\gamma,\gamma Z} \sim 10^{-27}$ cm^{3}s^{-1}, through the resonant annihilations via heavier CP-even (H_2) or CP-odd Higgs boson (A). Note that the resonant annihilation through CP-odd Higgs boson A can only take place if T_{ν_α} is complex, as otherwise the coupling among $A\,\tilde{\nu}_R^1\tilde{\nu}_R^{1*}$ vanishes. The CP-odd Higgs resonance avoids stringent constraints on $\langle\sigma v\rangle_{W^+W^-,ZZ}$ coming from continuum fluxes of gamma rays [§]. We found that it requires large values of $\mathcal{I}m(T_{\nu_\alpha})$ to obtain the desired cross-section for the di-photon final state. However, a dominantly CP-odd Higgs resonance falls short in accounting for the desired thermal relic abundance; and, more importantly, the viable parameter space has been ruled out by constraints from the continuum spectrum of γ rays. In particular, we found that annihilation cross-sections to the following final states are somewhat above the upper limits set by the Fermi-LAT for a NFW halo profile [37, 44], *viz.* (i) $\langle\sigma v\rangle(\tilde{\nu}_R^1\tilde{\nu}_R^1 \to b\bar{b}) \sim 10^{-23}$cm^3 s^{-1} and (ii) $\langle\sigma v\rangle(\tilde{\nu}_R^1\tilde{\nu}_R^1 \to ZH) \sim 10^{-23}$cm^3 s^{-1}.

Also, a significant left-right mixing in the lightest sneutrino states, which enhance the photon signal, is tightly constrained from the direct DM searches. Thus, in this extension of the MSSM, although $\tilde{\nu}_R^1$ is a viable DM candidate, achieving large $\langle\sigma v\rangle_{\gamma\gamma}$ seems to be incompatible with other constraints on DM.

B. $\tilde{\nu}_R$ and the NMSSM

Next we consider a similar extension of the scale invariant NMSSM, with three generations of right-handed neutrino superfields. The new superpotential becomes

$$W = W_{MSSM} + \lambda\widehat{S}\widehat{H}_u\cdot\widehat{H}_d + \frac{\kappa}{3}\widehat{S}^3 + y_\nu\,\hat{H}_u\cdot\hat{L}\,\hat{\nu}_R^c + \frac{y_r}{2}\,\hat{S}\,\hat{\nu}_R^c\,\hat{\nu}_R^c\,, \tag{10}$$

where W_{MSSM} denotes the MSSM superpotential without the μ term. The $\hat{S}$ denotes the singlet superfield that already appears in the NMSSM. When the scalar component of $\hat{S}$

[§] Note that a complex value for T_ν leads to a mixing among the CP-even and CP-odd Higgses in the mass eigen-basis.

gets a VEV of the order of electro-weak scale, μ term of correct size would be generated. Similarly, the right handed neutrinos also acquire an effective Majorana mass around the electro-weak values as long as the dimensionless coupling y_r is order one [62]. At the tree level the (3×3) light neutrino mass matrix, that arises via the seesaw mechanism, has a very well-known structure given by,

$$m_\nu^{tree} = -m_D M_R^{-1} m_D^T, \tag{11}$$

Unlike MSSM, here $y_\nu \sim \mathcal{O}(10^{-6})$ can reproduce the neutrino mass and mixing data [63]. As before, flavor mixings in the slepton sector can be induced radiatively by the off-diagonal entries in the neutrino Yukawa coupling, which are suppressed due to the smallness of Yukawa couplings. However, for simplicity we assume neutrino Yukawa couplings to be diagonal which alleviates the slepton flavor mixings completely. The soft-supersymmetry-breaking scalar potential is given by,

$$\begin{aligned} V_{soft} = V_{MSSM} + (T_\lambda\, H_u \cdot H_d\, S + \frac{1}{3} T_\kappa\, S^3 \\ + T_\nu\, H_u \cdot \tilde{L}\, \tilde{\nu}_R^c + T_r\, S\, \tilde{\nu}_R^c\, \tilde{\nu}_R^c + \text{h.c}) + m_{\tilde{\nu}_R}^2 |\tilde{\nu}_R^c|^2 + m_S^2 |S|^2 \ , \end{aligned}$$

where V_{MSSM} denotes the soft-supersymmetry breaking terms in the MSSM and $T_\nu \equiv T_{\nu_\alpha} y_{\nu_\alpha}$ where α denotes the generation indices. We do not assign VEV to $\tilde{\nu}_R^c$, thus R-parity is unbroken at the minimum of the scalar potential. In particular, the neutral scalar fields can develop, in general, the following vacuum expectation values at the minimum of the scalar potential.

$$\langle H_d^0 \rangle = v_d/\sqrt{2}; \ \ \langle H_u^0 \rangle = v_u/\sqrt{2}; \ \ \langle S \rangle = v_s/\sqrt{2} \ .$$

We further assume that y_r and T_r are flavor-diagonal for simplicity and consider the lightest $\tilde{\nu}_R^c$ as the lightest R-parity odd particle; and forefore the DM candidate.

We begin by decomposing the sneutrino fields in terms of real and imaginary components.

$$\begin{aligned} \tilde{\nu}_L &= \frac{1}{\sqrt{2}}(\phi_L + i\sigma_L), \\ \tilde{\nu}_R^c &= \frac{1}{\sqrt{2}}(\phi_R + i\sigma_R). \end{aligned} \tag{12}$$

where, ϕ_L, ϕ_R are the CP-even and σ_L, σ_R are the CP-odd scalar fields. The presence of $\Delta L = 2$ terms (for *e.g.* $y_r\, \hat{S}\, \hat{\nu}_R^c\, \hat{\nu}_R^c$) in the superpotential, and the corresponding soft-breaking term ($T_r\, \tilde{S}\, \tilde{\nu}_R^c\, \tilde{\nu}_R^c + \text{h.c.}$) can induce splitting between different CP-eigenstates of $\tilde{\nu}_R^c$.

The mass matrix for CP-even eigenstates (ϕ_L, ϕ_R) or for CP-odd eigenstates (σ_L, σ_R) is given by,

$$m^2_{\nu^{R,I}} = \begin{pmatrix} m^{R,I}_{11} & m^{R,I}_{12} \\ m^{R,I}_{21} & m^{R,I}_{22} \end{pmatrix}, \tag{13}$$

where,

$$\begin{aligned} m^{R,I}_{11} &= \frac{1}{8}(4v_u^2 y_\nu^2 + 8m_{\tilde{l}}^2 + (g_1^2+g_2^2)(-v_u^2+v_d^2)), \\ m^{R,I}_{12} &= m^{R,I}_{21} = \frac{1}{4}(2\sqrt{2}v_u T_\nu \pm v_s(\mp 2v_d\lambda y_\nu + 4v_u y_r y_\nu)), \\ m^{R,I}_{22} &= \frac{1}{4}(4m_R^2 + 8y_r^2 v_s^2 + 2y_\nu^2 v_u^2 \pm 2\Big((2\kappa v_s^2 - \lambda v_d v_u)y_r + 4\sqrt{2}T_r v_s - 2\lambda y_r v_u v_d)\Big). \end{aligned} \tag{14}$$

The mass matrices can be diagonalized by unitary matrices Z^I and Z^R,

$$\begin{aligned} Z^I m^2_{\nu^I} Z^{I,\dagger} &= {m^D_{\nu^I}}^2, \\ Z^R m^2_{\nu^R} Z^{R,\dagger} &= {m^D_{\nu^R}}^2, \end{aligned} \tag{15}$$

where $m^D_{\nu^I}$ and $m^D_{\nu^R}$ denote the diagonalized mass matrices respectively, and the corresponding mass eigenstates are denoted by σ_i and ϕ_i $(i \in \{1,2\})$; g_1 and g_2 are the $SU(2)_L$ gauge couplings; $m^2_{\tilde{l}}$ is the soft-supersymmetry breaking mass term for slepton doublet. The other parameters are described in Eqs. (10) and (12). Generically, ϕ_i and σ_i are non-degenerate, thanks to the $\Delta L = 2$ term present in the superpotential.

In general, lightest of the states σ_i or ϕ_i could be the lightest SUSY particle in different regions of the parameter space. Depending on the choice of the parameters, σ_i or ϕ_i can have dominant gauge and/or Yukawa interactions. Their mass difference, defined by $\Delta m = |m_{\phi_i} - m_{\sigma_i}|$ cannot be arbitrary, especially when σ_i and ϕ_i have dominant left-handed component, i.e., σ_i and ϕ_i are of $\tilde{\nu}_L$-type. In this case, the one-loop contributions to the neutrino mass matrix can be quite large which essentially limits $\Delta m \simeq 100$ keV [63, 78]. Moreover, due to its doublet nature under $SU(2)_L$, stringent constraints would also appear from the sneutrino-nucleus scattering (via t-channel Z boson exchange processes) [79].

On the other hand, aforementioned constraints can be evaded naturally, if we assume that ϕ_1 and σ_1 are dominantly right-handed. In fact these states are completely unconstrained, and their splitting can be traced back to $\Delta L = 2$ terms present in the mass matrix. However, nearly degenerate or degenerate σ_1 and ϕ_1 may be achieved, provided all $\Delta L = 2$ in

parameter	A	B	C	parameter	A	B	C
$\tan\beta$	2.9	9.0	10.0	μ_{eff}	322	-273.2	-269.3
κ	0.712	0.713	0.713	T_κ	-45.14	277.9	273.92
y_r^{33}	0.18	0.506	0.50	T_r^{33}	-36.10	-79.98	-80.11
λ	0.719	0.73	0.719	T_λ	418	-1077	-1077
$m_{\tilde{b_{1,2}}}$	3200	3200	3200	$m_{\tilde{Q}}$	2000	2000	2000
$m_{\tilde{l}}$	300	300	300	m_{H_1}	126	125.8	127
m_{H_2}	332	260.14	259.92	m_{H_3}	1893	1810	1903
m_{A_s}	269.7	456.7	452	m_{A_3}	1891	1807	1903
$m_{H^\pm}$	1887	1803	1897	$m_{\tilde{\nu_1^R}}$	135	304	305
$m_{\tilde{\chi}_1^\pm}$	197	201.6	196	$m_{\tilde{\nu_1^I}}$	135	130.6	130
$m_{\tilde{\chi}_1^0}$	177	179.6	179	$m_{\tilde{t_{1,2}}}$	3200	3200	3200
σ(DM DM $\to \gamma\gamma$) (10^{-27} cm^3 s^{-1})	2.0	2.0	1.3	$\Omega_{\phi_1,\sigma_1}h^2$	0.11	0.10	0.09

TABLE I. Benchmark points for σ_1 and/or ϕ_1 DM (co-) annihilation via (A) CP-odd Higgs pole; (B) CP-even Higgs pole with single component DM; and (C) CP-even Higgs pole with degenerate σ_1, σ_2 DM. All masses are shown in GeV.

combination vanishes. The condition for degeneracy, thus, can be expressed as,

$$\Big(\Big(-v_d v_u\lambda + v_s^2\kappa\Big)y_r + \sqrt{2}v_s T_r\Big) = 0. \tag{16}$$

Though, it seems a bit fine-tuned, we find that, potentially testable photon signals can be achieved. Based on the above facts, we consider the following possibilities for a 130-135 GeV $\tilde{\nu}_R$ type dark matter, as presented in Table I.

1. ϕ_1/σ_1 *Dark Matter*

In the first scenario, we illustrate how CP eigenstates ϕ_1 or σ_1 can annihilate through singlet-like CP-even Higgs (H_2) resonance to $\gamma\gamma$ (see Fig. 1). The singlet nature of H_2 helps to accommodate constraints from the continuum γ. In addition, the narrow width of a singlet–like H_2 also reduces the contribution of the resonance mediated channels to the

relic density.

The couplings $C_{r,o}$ in Eq. 3, between the singlet-like CP-even Higgs and ϕ_1/σ_1 takes the following form,

$$C_r \simeq \sqrt{2}T_r Z_{23}^H Z_{12}^{R\ 2} + v_s \left(2\kappa y_r + y_r^2\right) Z_{23}^H Z_{12}^{R\ 2} + \dots$$
$$C_o \simeq -\sqrt{2}T_r\ Z_{23}^H\ Z_{12}^{I\ 2} - v_s \left(2\kappa y_r - y_r^2\right) Z_{23}^H Z_{12}^{I\ 2} + \dots \tag{17}$$

The term proportional to T_r comes from the soft-supersymmetry breaking sector, while the other terms come from the F-term contributions to the scalar potential. Z^H represents the mixing matrix of the CP-even Higgs bosons. Assuming that the second lightest CP-even Higgs (singlet-like) boson contributes dominantly, Z_{23}^H is the relevant entry in Eq. 17 while the ellipsis indicate the sub-leading contributions originating from small doublet components. These couplings play crucial roles in determining both $\langle\sigma v\rangle_{\gamma\gamma}$ and the thermal relic abundance.

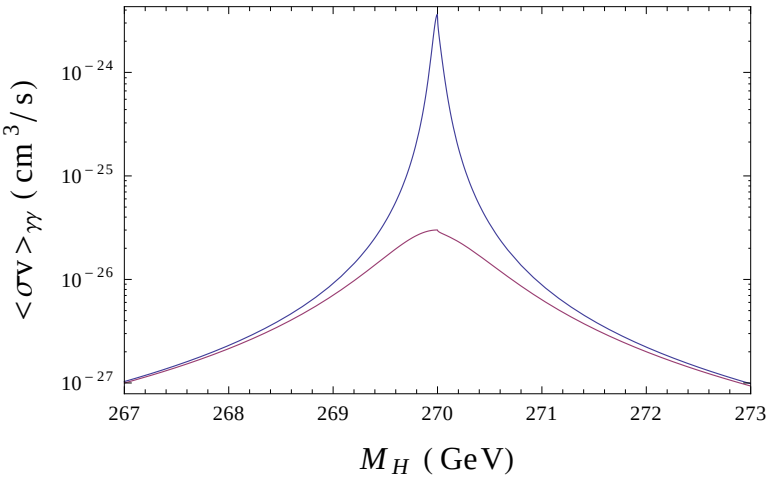

FIG. 2. The enhancement of the $\langle\sigma v\rangle_{\gamma\gamma}$ in the vicinity of the resonance, above and below the pole (270 GeV) is shown here. The blue curve represents a total width of 0.1 GeV below the threshold while the red curve represents a width of 1.1 GeV in the same region.

The desired signal $\langle\sigma v\rangle_{\gamma\gamma}$ can be easily enhanced with larger $C_{o/r}$ and/or λ. Larger values of λ can enhance the effective coupling of $H_2 - \gamma - \gamma$ via $\lambda H_2(S)\tilde{H}_u^{\ +}\tilde{H}_d^{\ -}$ loops in Eq. 10. Since the contribution from the charginos ($\chi^{\pm}$) running in the loop dominates, light higgsino–like $\chi^{\pm}$ are desired to enhance the signal. In Fig. 2, we present $\langle\sigma v\rangle_{\gamma\gamma}$ with representative values of the input parameters around the Higgs threshold. Interestingly, we

can easily obtain the $\langle\sigma v\rangle_{\gamma\gamma}$ with the pole mass below or above the threshold, i.e. $(2m_{\sigma_1/\phi_1})$. However, the correct thermal relic density can be obtained only when the pole is below the

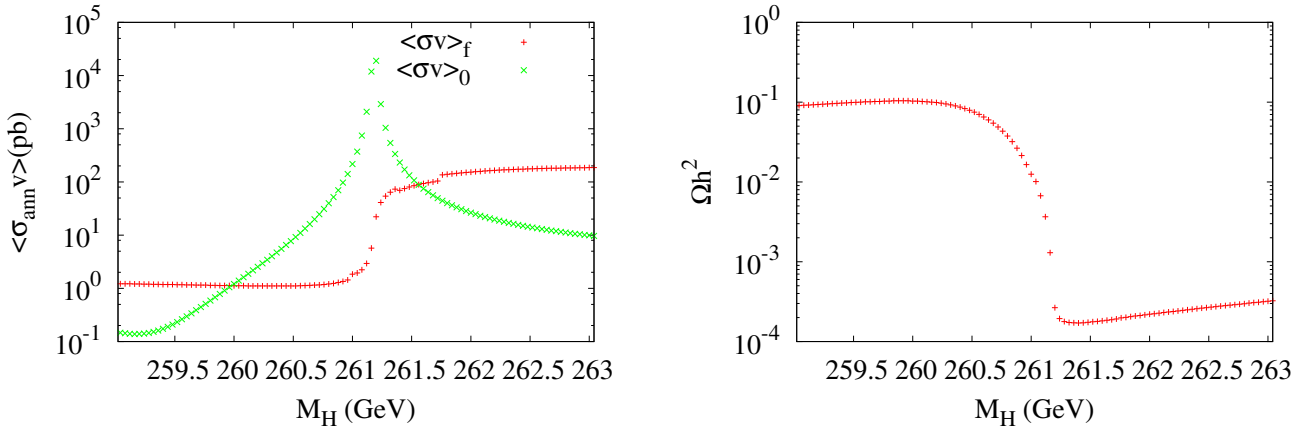

FIG. 3. Relic density of σ_1 DM, with a mass of 130.6 GeV, has been plotted against the singlet–like CP-even Higgs pole mass. In the left panel the thermally avaraged cross-sections at freeze-out temperature (T_f) and at late time (the speed of DM $v \sim 0.001$ or $T = T_0 \sim 10^{-4}$ GeV) have been shown in red and green respectively. In the right panel the CP-even Higgs mass is varied to demonstrate the relic abundance below and above the threshold (261.2 GeV). All other relevant parameters have been mentioned in column (B) of Table I.

threshold, as shown in the left panel of Fig. 3. To understand it better, we also depict the parameter x_f (i.e. m/T_f, as already discussed in Sec. II), which characterises the freeze-out, against M_H in the Fig. 4. As can be seen from Fig. 4, x_f is larger for M_H above the threshold (260 GeV), implying late freeze–out compared to the scenario when M_H is below the threshold. Therefore, in this region a lower relic density is obtained.

As noted in Eq. 17 and Eq. 14, both the couplings $C_{r,o}$, as well as the mass of σ_1, depend on T_r and y_r, while the other free parameters involved in these equations also affect, among others, the Higgs sector. Therefore, in Fig. 5, we present the allowed parameter space in the (T_r, y_r) plane; assuming the following input parameters (at the SUSY scale):

$$\lambda = 0.73,\ \kappa = 0.713,\ T_\lambda = -1077,\ T_\kappa = 277.92,\ \tan\beta = 10.$$

Our choice for these parameters are consistent with the LHC data on the SM-like CP-even Higgs while providing us with another singlet-like CP-even Higgs with a mass of 260 GeV.

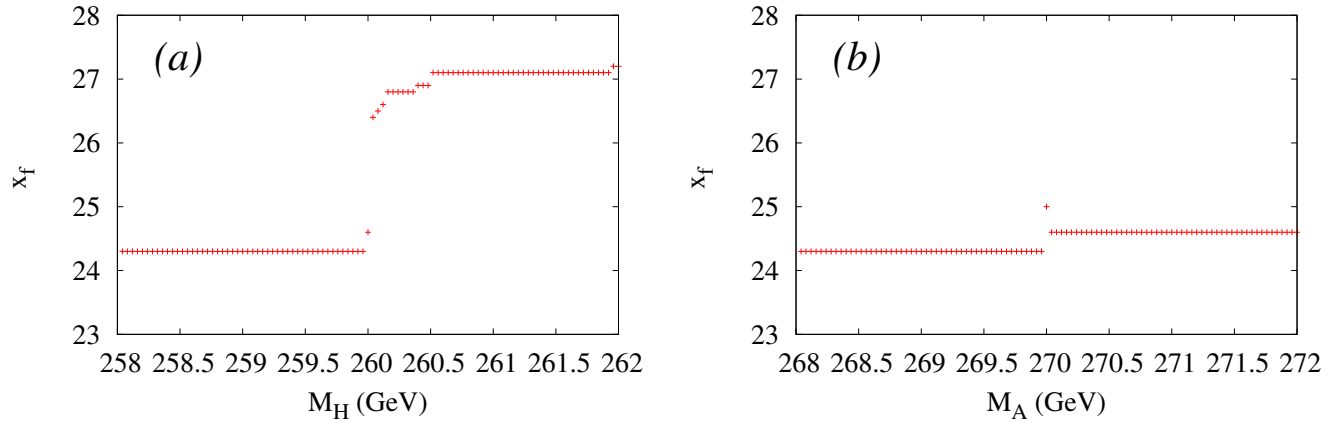

FIG. 4. $x_f = \frac{m_{\sigma_1}}{T_f}$, where σ_1 is dark matter, around the singlet–like (a) CP-even Higgs pole and (b) CP-odd Higgs pole have been plotted. Note that, for our benchmark points, m_{ϕ_1/σ_1} is 130 GeV (135 GeV) for the CP-even (CP-odd) Higgs resonance respectively. This figure depicts the late freeze-out of the DM when the mass of the DM is less than half of the CP-even/CP-odd Higgs mass, i.e. when the physical pole is encountered.

All other parameters are set to alleviate LHC constraints as mentioned in Sec. III. We also set soft breaking parameter of the right handed sneutrino so to have σ_1 as LSP with mass 130.5 GeV. With the given parameters, we obtain $m_{H_{SM}} = 125.7$ GeV while for the singlet like Higgs we get $m_{H_2} = 260.1$ GeV. Assuming, for simplicity, that the third generation right handed sneutrino as the LSP, we only varied T_r^{33} and y_r^{33} to deliniate the WMAP satisfied region in the vicinity of H_2 resonance. In this region, due to the singlet nature of H_2 and the smallness of the coupling among $\sigma_1 - H_2 - \sigma_1$, the annihilation channels mediated by the lightest CP-even Higgs boson contributes singnificantly in satisfying the relic density. These points are also allowed by the recent bounds from LUX [53]. Interestingly, the whole parameter space can provide with adequate cross-section for $\langle\sigma v\rangle_{\gamma\gamma}$.

For the benchmark point presented in column (B) of Table I, we assume σ_1 to be the DM.[¶] The representative values, as shown in column (B) of Table I satisfy the desired $\langle\sigma v\rangle_{\gamma\gamma}$ and other mentioned constraints including WMAP. In the calculation of $\langle\sigma v\rangle_{\gamma\gamma}$, we

[¶] Note that by simply reversing the signs of y_r and T_r, one can have CP-even ϕ_1 as the LSP while the mass spectra remains unchanged. Consequently, one can explain the observed γ signal with CP-even ϕ_1 DM.

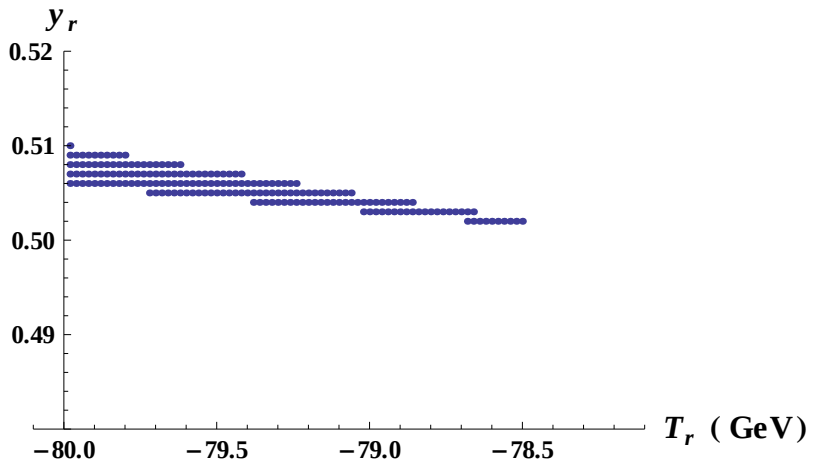

FIG. 5. WMAP allowed parameter space for σ_1 DM, with a mass of 130 GeV, has been shown in the T_r, y_r plane. All these points satisfy direct detection limits from LUX while having adequate cross-section to account for the photon signal.

have $\mathrm{Br}(\mathrm{H}_2 \to \gamma\gamma) = 1.5 \times 10^{-4}$, $\Gamma_H = 0.02$ GeV and $\delta = 0.007$ (see Eq. 3). We also consider another simple scenario, where σ_1 is not the sole component of the dark matter density. For example, if the second lightest CP-odd sneutrino eigenstates, σ_2 is degenerate with σ_1, then it will be present during the time of decoupling to contribute to the relic abundance. An example is depicted in column (C) of Table I which possesses the desired values of the thermal relic density and $\langle\sigma v\rangle_{\gamma\gamma}$.

2. *Degenerate ϕ_1-σ_1 Dark Matter*

Both of these components can be present today, if their masses are (near) degenerate[**]. In this case, this degenerate DM annihilates through singlet-like CP odd Higgs (A_s) resonance to $\gamma\gamma$, as illustrated in Fig. 1. Similar to the previous case, a singlet–like CP-odd Higgs, with dominant branching ratio to di-photon final state, helps in satisfying the continuum constraints; while enhancing DM annihilation cross-section to di-photon final state in the vicinity of the narrow resonance. To estimate $\langle\sigma v\rangle_{\gamma\gamma}$, as mentioned, we use Eq. 3. The coupling C of the singlet–like CP-odd Higgs (A_s) with $\sigma_1 - \phi_1$, in the gauge eigen-basis, is

[**] Mass splitting Δ_m between ϕ_1,σ_1 should be $\mathcal{O}(100$ keV), so that the heavier state is sufficiently long-lived.

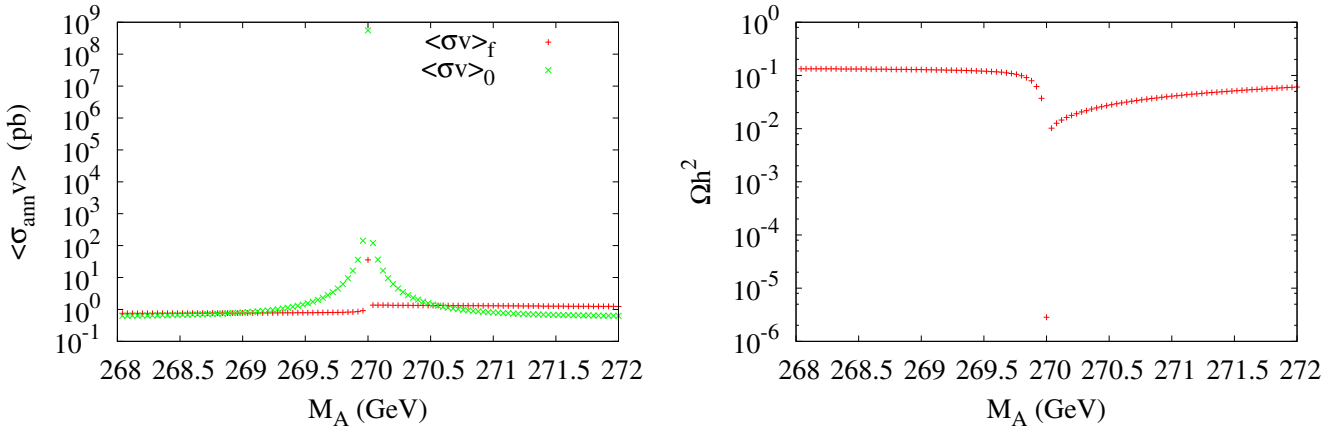

FIG. 6. Relic density of mixed $\phi_1,\ \sigma_1$ type DM with a mass of 135 GeV, has been plotted against the singlet–like CP-odd Higgs pole mass. In the left panel the thermally avaraged cross-sections at freeze-out temperature (T_f) and at late time (the speed of DM $v \sim 0.001$ or $T = T_0 \sim 10^{-4}$ GeV) have been shown in red and green respectively. In the right panel the CP-odd Higgs mass is varied to demonstrate the relic abundance below and above the threshold (270 GeV).

given by,

$$C = -2\kappa v_s y_r Z^A_{s3} Z^I_{12} Z^R_{12} - \sqrt{2} Z^A_{s3} T_r Z^I_{12} Z^R_{12}; \tag{18}$$

where, Z^A denotes the mixing matrices of the CP-odd Higgs and all other symbols are as defined before.

As in the previous case, $\langle\sigma v\rangle_{\gamma\gamma}$ can easily be enhanced by increasing C (thus y_r and/or λ), but that could lead to small relic abundance. A light higgsino–like $\chi^\pm$ is desired to enhance the same. Again, we consider $m_{A_s} < 2m_{\phi_1-\sigma_1}$, i.e., part of the parameter space where the pole of the propagator is below the threshold, to obtain the right thermal relic abundance. In particular, here we require extremely singlet like pseudo-scalar Higgs so that $\text{Br}(A_s \to \gamma\gamma)$ (see Eq. 3) can be very large to account for the desired $\langle\sigma v\rangle_{\gamma\gamma}$. Also, the coupling C should be small so that the correct relic abundance can be obtained through the processes mediated by the other Higgs states. This in turn prefers small values of y_r if one does not want to have unnatural cancellation among different parameters in Eq. 18. However, here for $\delta > 0$ (see Sec. II), below the threshold, in our region of interest, we find A_s dominantly decays to a pair of ν_R which can substancially enhance the decay width of A_s. It also affects the DM density as DM can also annihilate in to a pair of ν_R via A_s resonance leading to a small relic

density. To circumvent this problem, we add an additional Majorana mass term ($m_N \nu_R \nu_R$) to the Lagrangian which enhance the masses for sterile neutrinos to kinematically forbids this decay channel. Thus the pole can appear very close to the threshold and $\langle \sigma v \rangle_{\gamma\gamma}$ can be extremely large in this region (as the branching fraction $A_s \to \gamma\gamma$ can be as large as ∼70%).

To demonstrate our results, we present in the left panel of Fig. 6, the thermally averaged cross-section, when the pole falls above the threshold (270 GeV), is a little larger than the same when the pole falls below the threshold. Also, as the right panel of Fig. 6 shows, in the former case, freeze-out happens a little later. Consequently, the thermal relic abundance decreases in the former case. Note that, due to the much smaller width of A_s compared to that of H_2 in the previous case, the effect of the resonance on the relic density is quite small.

A benchmark point in column (A) of Table I has been presented to summarize the results. The relic density can be obtained mainly via the annihilation channels mediated via the off-shell CP-even Higgs bosons. In the calculation of $\langle \sigma v \rangle_{\gamma\gamma}$, we have $\mathrm{Br}(\mathrm{A_s} \to \gamma\gamma) \simeq 5 \times 10^{-4}$, $\Gamma_{A_s} = 0.003$ GeV and $\delta = 0.002$. All phenomenological constraints, from both direct and indirect detection data, can easily be satisfied for the benchmark point (A) shown in Table I, thanks to the singlet nature of A_s.

3. *Constraints from direct detection*

An interesting issue for the models, which give the desired $\langle \sigma v \rangle_{\gamma\gamma}$, is to address constraints coming from the spin-independent direct detection, particularly in the light of XENON-100 and LUX data. In the NMSSM, the parameter space for a 130-135 GeV neutralino DM, achieving the desired $\langle \sigma v \rangle_{\gamma\gamma}$, is constrained by the present bound $\sigma(p)_{SI} \lesssim 1.2 \times 10^{-8}$ pb and $\sigma_{SI} \lesssim 1.5 \times 10^{-9}$ pb for $M_{DM} \sim 130 - 135$ GeV from XENON-100 [52] and LUX [53] respectively. An important issue concerns the quark coefficient in the nucleon which may lead to large theoretical uncertainty in the calculation. In this work, we always keep the default values that are used in `micrOMEGAs-3`.

Being a real scalar, ϕ_1 (σ_1) interacts with nucleons via Higgs exchange processes. As the Yukawa coupling is very small ($\sim 10^{-7}$), the coupling $\phi_1/\sigma_1 - H - \phi_1/\sigma_1$ is principally determined by $T_r S \tilde{\nu}_R^c \tilde{\nu}_R^c$ and $\kappa v_s S^* \tilde{\nu}_R^c \tilde{\nu}_R^c$, $\lambda y_r v_{u,d} H_{d,u}^* \tilde{\nu}_R^c \tilde{\nu}_R^c$ terms, arising from the soft-breaking sector and the F-term contributions respectively. Singlet–like Higgs does not couple to the quarks or gluons at tree–level, while the coupling of the doublet–like Higgs with $\tilde{\nu}_R^c \tilde{\nu}_R^c$

is quite small. Also, since both ϕ_1 and σ_1 are dominantly right-chiral, Z boson exchange does not lead to large $\sigma(p)_{SI}$ even when these are degenerate. The only term, which gives rise to dominant contribution to $\sigma(p)_{SI}$ originates from the F-term contribution $(\lambda\frac{y_r}{2}\tilde{\nu}^c_R\tilde{\nu}^c_R H_u.H_d +$ h.c). While both λ and y_r appears in $\langle\sigma v\rangle_{\gamma\gamma}$, note that it is possible to achieve large $\langle\sigma v\rangle_{\gamma\gamma}$ with small y_r by increasing the soft-term T_r appropriately. In summary, the scenarios proposed here are not significantly constrained by the XENON-100, these are moderately constrained by the LUX data.

IV. SUMMARY AND CONCLUSIONS

We have explored the possibility that the annihilation of 130-135 GeV right-chiral sneutrino DM into two photons can produce the observed line-like feature in the Fermi-LAT data. In this context, we examine the candidature of right-sneutrino dark matter – a scenario that can have somewhat unusual phenomenological implications. It is, however, seen that the augmentation of the MSSM just with right-chiral neutrino superfields is inadequate. The difficulty arises from severe constraints on various annihilation channels of the dark matter, most notably into ZH and $b\bar{b}$, derived from the continuum flux of photons. However, in the extension of the next-to-minimal model (NMSSM), annihilating right-chiral sneutrino DM, can produce the observed line feature. Due to the extra singlet field present in this model, a singlet–like CP-odd or CP-even Higgs boson resonance produces adequate annihilation cross-section to fit the observation. We find that in case of a CP-odd Higgs resonance, one needs the lightest CP-even and the lightest CP-odd right-chiral sneutrino states to be (almost) degenerate. In the latter case however, this is not a requirement. We present a few benchmark points to substantiate our claims and highlight the spectrum which is consistent with the data. While our benchmark points also satisfy the present direct detection bounds, improved bounds in near future may be able to explore the viability of our scenario. In addition, we show that when the pole in the resonance is a little below twice the mass of the DM, the thermal production of right-chiral sneutrino dark matter can be sufficient to also account for the DM abundance, as required by the CMBR data, especially in the case of degeneracy in the sneutrino sector.

V. ACKNOWLEDGEMENT

AC and DD would like to thank Florian Staub for useful discussions about the code SARAH. The work of AC, BM and SKR was partially supported by funding available from the Department of Atomic Energy, Government of India, for the Regional Centre for Accelerator-based Particle Physics (RECAPP), Harish-Chandra Research Institute (HRI). DD acknowledges support received from the DFG, project no. PO-1337/3-1 at the Universität Würzburg. DD thanks RECAPP, Allahabad, for hospitality during the initial part of the proejct.

---

[1] W. B. Atwood *et al.* [LAT Collaboration], Astrophys. J. **697**, 1071 (2009), [arXiv:0902.1089].

[2] T. Bringmann, X. Huang, A. Ibarra, S. Vogl and C. Weniger, JCAP **1207**, 054 (2012), [arXiv:1203.1312].

[3] C. Weniger, JCAP **1208**, 007 (2012), [arXiv:1204.2797].

[4] E. Tempel, A. Hektor and M. Raidal, JCAP **1209**, 032 (2012) [Addendum-ibid. **1211**, A01 (2012)], [arXiv:1205.1045].

[5] M. Su and D. P. Finkbeiner, [arXiv:1206.1616].

[6] A. Hektor, M. Raidal and E. Tempel, Astrophys. J. **762**, L22 (2013), [arXiv:1207.4466].

[7] M. Su and D. P. Finkbeiner, [arXiv:1207.7060].

[8] D. Hooper and T. Linden, Phys. Rev. D **86**, 083532 (2012), [arXiv:1208.0828].

[9] N. Mirabal, Mon. Not. Roy. Astron. Soc. **429**, L109 (2013), [arXiv:1208.1693].

[10] A. Hektor, M. Raidal and E. Tempel, [arXiv:1208.1996].

[11] H. -S. Zechlin and D. Horns, JCAP **1211**, 050 (2012), [arXiv:1210.3852].

[12] A. Rajaraman, T. M. P. Tait and D. Whiteson, JCAP **1209**, 003 (2012), [arXiv:1205.4723].

[13] T. Bringmann and C. Weniger, Phys. Dark Univ. **1**, 194 (2012), [arXiv:1208.5481].

[14] S. Profumo and T. Linden, JCAP **1207**, 011 (2012), [arXiv:1204.6047].

[15] A. Boyarsky, D. Malyshev and O. Ruchayskiy, [arXiv:1205.4700].

[16] A. Albert et. al. [Fermi-LAT collaboration], [arXiv:1305.5597].

[17] J. M. Cline, Phys. Rev. D **86**, 015016 (2012), [arXiv:1205.2688].

[18] H. M. Lee, M. Park and W. -I. Park, Phys. Rev. D **86**, 103502 (2012), [arXiv:1205.4675].

[19] E. Dudas, Y. Mambrini, S. Pokorski and A. Romagnoni, JHEP **1210**, 123 (2012), [arXiv:1205.1520].

[20] K. -Y. Choi and O. Seto, Phys. Rev. D **86**, 043515 (2012), [Erratum-ibid. D **86**, 089904 (2012)], [arXiv:1205.3276].

[21] B. Kyae and J. -C. Park, Phys. Lett. B **718**, 1425 (2013), [arXiv:1205.4151].

[22] B. S. Acharya, G. Kane, P. Kumar, R. Lu and B. Zheng, [arXiv:1205.5789].

[23] M. R. Buckley and D. Hooper, Phys. Rev. D **86**, 043524 (2012), [arXiv:1205.6811].

[24] X. Chu, T. Hambye, T. Scarna and M. H. G. Tytgat, Phys. Rev. D **86**, 083521 (2012), [arXiv:1206.2279].

[25] N. Weiner and I. Yavin, Phys. Rev. D **86**, 075021 (2012), [arXiv:1206.2910].

[26] J. H. Heo and C. S. Kim, Phys. Rev. D **87**, 013007 (2013), [arXiv:1207.1341].

[27] M. T. Frandsen, U. Haisch, F. Kahlhoefer, P. Mertsch and K. Schmidt-Hoberg, JCAP **1210**, 033 (2012), [arXiv:1207.3971].

[28] J. -C. Park and S. C. Park, Phys. Lett. B **718**, 1401 (2013), [arXiv:1207.4981].

[29] S. Tulin, H. -B. Yu and K. M. Zurek, $\gamma\gamma$," [arXiv:1208.0009].

[30] J. M. Cline, G. D. Moore and A. R. Frey, Phys. Rev. D **86**, 115013 (2012), [arXiv:1208.2685].

[31] L. Bergstrom, Phys. Rev. D **86**, 103514 (2012), [arXiv:1208.6082].

[32] N. Weiner and I. Yavin, Phys. Rev. D **87**, 023523 (2013), [arXiv:1209.1093].

[33] J. Fan and M. Reece, [arXiv:1209.1097].

[34] H. M. Lee, M. Park and W. -I. Park, JHEP **1212**, 037 (2012), [arXiv:1209.1955].

[35] L. Wang and X. -F. Han, Phys. Rev. D **87**, 015015 (2013), [arXiv:1209.0376].

[36] F. D'Eramo, M. McCullough and J. Thaler, [arXiv:1210.7817].

[37] N. Bernal, C. Boehm, S. Palomares-Ruiz, J. Silk and T. Toma, [arXiv:1211.2639].

[38] Y. Farzan and A. R. Akbarieh, [arXiv:1211.4685].

[39] Y. Bai and J. Shelton, JHEP **1212**, 056 (2012), [arXiv:1208.4100].

[40] D. Das, U. Ellwanger and P. Mitropoulos, JCAP **1208**, 003 (2012), [arXiv:1206.2639].

[41] W. Buchmuller and M. Garny, JCAP **1208**, 035 (2012), [arXiv:1206.7056].

[42] I. Cholis, M. Tavakoli and P. Ullio, Phys. Rev. D **86**, 083525 (2012), [arXiv:1207.1468].

[43] T. Cohen, M. Lisanti, T. R. Slatyer and J. G. Wacker, JHEP **1210**, 134 (2012), [arXiv:1207.0800].

[44] X. -Y. Huang, Q. Yuan, P. -F. Yin, X. -J. Bi and X. -L. Chen, JCAP **1211**, 048 (2012), [arXiv:1208.0267].

[45] G. Chalons, M. J. Dolan and C. McCabe, [arXiv:1211.5154].

[46] T. Basak and S. Mohanty, JHEP **1308**, 020 (2013), [arXiv:1304.6856].

[47] G. Tomar, S. Mohanty and S. Rao, [arXiv:1306.3646].

[48] T. Basak and T. Mondal, [arXiv:1308.0023].

[49] F. Boudjema, A. Semenov and D. Temes, Phys. Rev. D **72**, 055024 (2005), [hep-ph/0507127].

[50] F. Ferrer, L. M. Krauss and S. Profumo, Phys. Rev. D **74** (2006) 115007, [hep-ph/0609257].

[51] G. Chalons and A. Semenov, JHEP **1112**, 055 (2011), [arXiv:1110.2064].

[52] E. Aprile *et al.* [XENON100 Collaboration], Phys. Rev. Lett. **109**, 181301 (2012), [arXiv:1207.5988].

[53] D.S. Akerib et. al. [LUX collaboration], [arXiv:1310.8214].

[54] B. Shakya, Phys. Dark Univ. **2**, 83 (2013), [arXiv:1209.2427].

[55] E. Komatsu *et al.* [WMAP Collaboration], Astrophys. J. Suppl. **192** (2011) 18, [arXiv:1001.4538].

[56] T. Asaka, K. Ishiwata and T. Moroi, Phys. Rev. D **73**, 051301 (2006), [arXiv: hep-ph/0512118].

[57] T. Asaka, K. Ishiwata and T. Moroi, Phys. Rev. D **75**, 065001 (2007), [arXiv: hep-ph/0612211].

[58] S. Gopalakrishna, A. de Gouvea and W. Porod, JCAP **0605**, 005 (2006) [hep-ph/0602027].

[59] D. Choudhury, S. K. Gupta, B. Mukhopadhyaya, Phys. Rev. D **78**, 015023 (2008), [arXiv:0804.3560]; S. K. Gupta, B. Mukhopadhyaya, S. K. Rai, Phys. Rev. D **75**, 075007 (2007), [arXiv: hep-ph/0701063];

S. Biswas, B. Mukhopadhyaya, Phys. Rev. D **81**, 015003 (2010), [arXiv:0910.3446];

S. Biswas, B. Mukhopadhyaya, Phys. Rev. D **79**, 115009 (2009), [arXiv:0902.4349].

[60] S. Banerjee, P. S. Bhupal Dev, S. Mondal, B. Mukhopadhyaya S. Roy, JHEP **1310** (2013) 221, [arXiv:1306.2143];

P. S. Bhupal Dev, S. Mondal, B. Mukhopadhyaya S. Roy, JHEP **1209** (2012) 110, [arXiv:1207.6542].

[61] V. De Romeri and M. Hirsch, JHEP **1212**, 106 (2012) [arXiv:1209.3891 [hep-ph]].

[62] R. Kitano and K. y. Oda, Phys. Rev. D **61**, 113001 (2000), [arXiv:hep-ph/9911327].

[63] D. Das and S. Roy, Phys. Rev. D **82**, 035002 (2010), [arXiv:1003.4381].

[64] D. G. Cerdeno, C. Munoz and O. Seto, Phys. Rev. D **79**, 023510 (2009), [arXiv:0807.3029].

[65] D. G. Cerdeno and O. Seto, JCAP **0908**, 032 (2009), [arXiv:0903.4677].

[66] D. G. Cerdeno, J. -H. Huh, M. Peiro and O. Seto, JCAP **1111**, 027 (2011), [arXiv:1108.0978].

[67] K. Huitu, J. Laamanen, L. Leinonen, S. K. Rai and T. Ruppell, JHEP **1211** (2012) 129, [arXiv:1209.6302].

[68] P. Gondolo and G. Gelmini , Nuclear Physics B **360**, 145, (1991).

[69] M. Ibe, H. Murayama, T. Yanagida, Phys.Rev.D **79** 095009 (2009), [arXiv:0812.0072].

[70] W. Guo and Y. Wu, Phys. Rev. D **79** 055012 (2009).

[71] G. Belanger, F. Boudjema, A. Pukhov and A. Semenov, Comput. Phys. Commun. **176**, 367 (2007) [arXiv:hep-ph/0607059]; G. Belanger, F. Boudjema, A. Pukhov and A. Semenov, Comput. Phys. Commun. **180** (2009) 747 [arXiv:0803.2360 [hep-ph]]; G. Belanger, F. Boudjema, A. Pukhov, A. Semenov, [arXiv:1305.0237].

[72] M. Ackermann *et al.* [LAT Collaboration], [arXiv:1205.2739].

[73] M. Ackermann *et al.* [Fermi-LAT Collaboration], Phys. Rev. Lett. **107** (2011) 241302, [arXiv:1108.3546].

[74] O. Adriani *et al.* [PAMELA Collaboration], Phys. Rev. Lett. **105** (2010) 121101, [arXiv:1007.0821].

[75] F. Staub, Comput. Phys. Commun. **184**, 1792 (2013).

[76] W. Porod, Comput. Phys. Commun. **153**, 275 (2003); W. Porod and F. Staub, Comput. Phys. Commun. **183**, 2458 (2012).

[77] A. Belyaev, N. Christensen, A. Pukhov, Comput. Phys. Commun. **184**, 1729 (2013).

[78] Y. Grossman and H. E. Haber, Phys. Rev. Lett. **78**, 3438 (1997), [arXiv: hep-ph/9702421].

[79] T. Falk, K. A. Olive and M. Srednicki, Phys. Lett. B **339**, 248 (1994), [arXiv: hep-ph/9409270].